WORLD CONFERENCE ON TIMBER ENGINEERING 2025
BRISBANE, AUSTRALIA
Advancing Timber for the Future Built Environment

DEVELOPMENT AND SEISMIC DESIGN OF NOVEL HYBRID TIMBER-STEEL ECCENTRICALLY BRACED FRAMES

Abebaw A. Mekonnen[1], Mairvat Abdulhamid[1], Matiyas A. Bezabeh[1], Colin A. Rogers[1], Alexander Salenikovich[2]

ABSTRACT: The development of a novel hybrid timber-steel eccentrically braced frame (TS-EBF) that offers significant advantages in both seismic performance and sustainability is presented herein. This novel seismic force-resisting system (SFRS) combines the increased lateral stiffness and environmental benefits of timber-braced frames with the outstanding energy dissipation capacity of steel links, thereby enhancing overall seismic resilience. The system employs structural steel for deformation-controlled elements (ductile links) and engineered wood products for force-controlled elements (beams, columns, and diagonal braces). To assess the performance of this system, a six-storey archetype building was designed using the direct displacement-based seismic design approach, taking into account the seismic conditions of Victoria, British Columbia, Canada. A fiber-based numerical model for ductile links was developed in *OpenSeesPy* and validated with existing experimental data. This validated model was then incorporated into a two-dimensional numerical model of the six-storey archetype building, enabling seismic performance assessment through nonlinear static and nonlinear response history analyses. A set of thirty-three hazard-consistent ground motion records, representative of the region's seismic characteristics, was selected for the analysis. Overall, the effectiveness of the TS-EBF system is demonstrated, highlighting its potential as a viable alternative SFRS for high-seismic risk regions in Canada.

KEYWORDS: Ductile links, Perforated web links, Seismic-force-resisting systems, Timber-steel hybrid buildings, direct displacement-based seismic design

1 – INTRODUCTION

Recent advancements in engineered wood products (EWP), such as glued-laminated timber (Glulam), cross-laminated timber (CLT), and structural composite lumber, have significantly improved the structural strength and stiffness, dimensional stability, and fire resistance of timber construction. As a result, many countries are embracing EWPs for mid- and high-rise buildings to meet the growing demand for housing in cities and as part of their net-zero emission strategies. The trend toward taller timber buildings increases the demand from lateral loads, such as seismic and wind forces, necessitating more advanced structural systems. Moreover, the recent update of the Canadian seismic hazard model has raised the seismic demand by up to 50%. Consequently, high-performance and resilient structural systems are required to withstand the increased lateral load demands associated with building height. Traditional timber constructions, which rely on the inelastic response of ductile connections to dissipate seismic energy, may not be an efficient option for these elevated demands [1]. In addition, permanent deformations resulting from the inelastic response of connections are very difficult to repair, significantly hindering the restoration of building functionality after seismic events. Systems that incorporate easily replaceable yielding elements are emerging as the most promising alternative to restore functionality quickly and cost-effectively. In these systems, replaceable yielding elements are strategically designed for simple removal and replacement, while connections and other unreachable components are maintained in an elastic state, eliminating the need for repair.

Timber-steel hybrid systems offer an effective solution for developing high-capacity seismic force-resisting systems (SFRS), while enabling easy implementation of replaceable yielding elements. Timber-steel hybrid systems integrate steel and timber members, maximizing structural efficiency by utilizing steel's ductility and strength alongside timber's sustainability and lightweight properties. Steel is used for deformation-controlled elements of the SFRS due to its high ductility. It enables the SFRS to experience inelastic deformations and dissipate seismic energy during severe seismic events. On the other hand, EWPs are used for force-controlled elements, which are designed to remain essentially elastic. Timber-steel hybridization can be at the component, system, or building level [2]. Component-level hybridization involves the combination of two or more materials within a single structural member, such as timber-encased buckling-restrained braces (BRB), columns consisting of an H-shaped steel section encased with glulam, and flitch sandwich beams. System-level hybridization encompasses members with different materials in a single system. Gohlich et al. [3] developed

[1] Department of Civil Engineering, McGill University, Montréal, Québec, Canada.

[2] Département des sciences du bois et de la forêt, Université Laval, Québec, Canada.

 https://doi.org/10.52202/080513-0369

a hybrid timber-steel moment-resisting frame (MRF) using replaceable steel links at the ends of glulam beams and column panel zones. Their results showed that the new hybrid timber-steel MRF achieved performance levels comparable to its steel counterpart with significantly lower foundation forces. Dong et al. [4] studied the performance of steel BRBs combined with glulam frames. Moerman et al. [5] used steel links as couplers in a coupled CLT shear wall. Steel MRFs are also combined with light timber frames or CLT to increase the lateral stiffness of the MRF. In addition to conventional steel, hybridization with special materials, including foundation isolators, viscoelastic, friction and hysteretic dampers are also used to improve the seismic performance of timber structures. Building-level hybridization involves integrating different structural systems composed of various materials within a single building. This approach has been widely applied in numerous projects, where concrete core walls or steel frames serve as the SFRS, whereas a glulam frame and CLT slab assembly are used as the gravity system.

Although various timber-steel hybrid systems have been developed, the general acceptance of timber construction in high-seismic regions and high-rise buildings remains limited. Most high-rise structures continue to rely on steel or concrete core walls as SFRSs, underlining the need for alternative solutions that enhance both seismic resilience and sustainability. To address these challenges, innovative hybrid systems are needed to harness the advantages of timber while providing sufficient ductility, stiffness, and energy dissipation to meet the demands of mid- and high-rise buildings in high-seismic regions. Acknowledging this need, several initiatives in Canada are promoting the use of timber-steel hybrid building constructions. As part of this initiative, funded by the Quebec Ministry of Natural Resources and Forests, the authors of this paper are developing the next generation of novel timber hybrid building systems. A novel hybrid timber-steel eccentrically braced frame (TS-EBF) is introduced in this paper with the objective of enhancing the seismic resilience of hybrid timber buildings. By incorporating steel links, the TS-EBF offers a replaceable energy dissipation mechanism while preserving the sustainability, aesthetic, lightweight, and other benefits of timber construction. The system development is first presented, followed by a direct displacement-based seismic design (DDBD) procedure adapted for TS-EBFs. Finally, a seismic performance evaluation of a case study building comprising a TS-EBF SFRS is investigated using nonlinear static analysis (NLSA) and nonlinear response history analysis (NLRHA) to evaluate the system's effectiveness.

2 – TIMBER-STEEL HYBRID EBF

Steel eccentrically braced frames (EBFs) are efficient SFRSs, with their performance demonstrated experimentally [6, 7] and during actual earthquakes [8]. In an EBF system, the line of action of two braces or a brace and a column is purposely offset to create a segment of the beam called a link that dissipates energy through controlled and stable plastic deformation under severe seismic events. Although EBFs have demonstrated good performance during earthquakes, restoring them to full functionality requires significant reconstruction, repairs, or even partial demolition [8]. The replaceable link concept, isolating the ductile component of the system from the elastic part of the SFRS, enables easy replacement of damaged links after an earthquake. It reduces downtime and associated costs by eliminating the need for extensive cutting and removal of damaged homogeneous links, enabling faster repairs and quicker return to operation. This concept also establishes a foundation for hybridizing the EBF system with timber, resulting in a sustainable and robust timber-steel hybrid structural system, timber steel hybrid EBF (TS-EBF).

In the proposed TS-EBF system, steel and timber are systematically combined to maximize the benefits of both materials. The link, which serves as the primary energy dissipation component, is made of ductile steel, whereas the force-controlled members consist of EWPs such as glulam, laminated veneer lumber (LVL), or parallel strand lumber (PSL). In this system, plastic deformations are confined to the steel link. The remaining force-controlled members and their connections are capacity-protected, ensuring that they stay elastic during seismic events. This facilitates the replacement of damaged links after earthquakes and enables the reuse of force-controlled elements, thereby enhancing the resilience and sustainability of the structure.

Figure 1 shows a schematic of a symmetrical chevron bracing TS-EBF configuration with a horizontal link, depicted in both its undeformed (Figure 1a) and deformed positions (Figure 1b). The links can also be configured vertically, where they are not an integral part of the beam, or horizontally, where they connect directly to the columns. In the latter case, the link-to-column connection is subjected to significant moment and shear forces, increasing its susceptibility to brittle fracture. Therefore, it is recommended to avoid such configurations [9]. The symmetrical chevron bracing configuration (Figure 1a) is subjected to limited or no axial forces, and the frame exhibits higher lateral stiffness [10]. A two-dimensional numerical model of the TS-EBF system, which will be explained in Section 3, is also shown in Figure 1c.

https://doi.org/10.52202/080513-0369

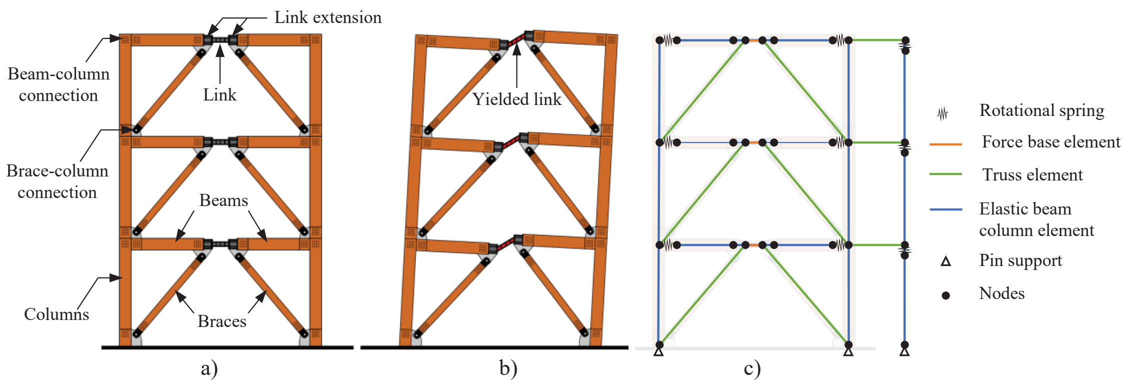

Figure 1. Timber-steel hybrid eccentrically braced frame (TS-EBF) a) undeformed, b) deformed and c)2D OpenseesPy model

2.1 LINKS OF TS-EBF SYSTEM

The steel link plays a critical role in achieving the desired seismic performance by distributing axial forces from the bracing to the column or other bracing through shear and bending action [11]. It acts as a structural fuse and protects the rest of the structure through plastic deformation during severe earthquake events. Based on the dominant force triggering plastic deformation, links are classified as shear links, where yielding is primarily due to shear; flexural links, where yielding is driven by bending; or intermediate links, which exhibit a combination of both shear and flexural yielding. Among these, shear links are preferred due to their ability to yield uniformly across the web, resulting in a high energy dissipation capacity. This superior performance has been confirmed through experimental studies [6,7,11]. The advantages of shear links are also recognized in major design codes, including CSA S16-24 [12], AISC 341-22 [13] and Eurocode 8-2004 [14] which all impose a stringent plastic rotation limit of 0.02 radians for flexural links, whereas the shear links are permitted a more lenient limit of 0.08 radians. Hence shear links are recommended to be used for TS-EBFs.

To protect the elastic EWP members and to ensure that plastic deformation remains confined to the steel link, it is critical to accurately predict the maximum forces generated by a fully yielded and strain-hardened link. Traditionally, an overstrength factor of 1.5 has been used to estimate these forces. However, a comprehensive review of twenty-five experimental studies presented in Azad and Topkaya [7] revealed that this value is a reasonable upper bound for long links; it overestimates the maximum shear force for some intermediate links and significantly underestimates it for very short links. These discrepancies were attributed to factors such as the shear contribution of the flanges, axial restraints resulting from nonlinear geometric effects, and excessive cyclic hardening of steel due to large plastic strains. CSA S16-24 [12] recommends an overstrength factor of $1.3R_y$ for wide-flange and modular links and $1.45R_y$ for built-up tubular cross-sections, where R_y is the ratio of nominal to minimum specified yield stress. Furthermore, standard W-section links require web stiffeners and follow section compactness criteria to avoid premature web buckling [15]. CSA S16-24 [12] recommends using Class 1 web and flange sections, but Class 2 flanges are also permitted for short links. In the current study, the CSA S16-24 [12] guidelines were followed to detail the links and determine their capacity.

Furthermore, the significant strength difference between steel and timber presents a key challenge in the TS-EBF system. When links are designed based on conventional steel EBF principles, they often require oversized timber members to maintain the intended yielding sequence, leading to inefficient and impractical designs. To address this issue, it is essential to reduce the yield capacity of steel links, ensuring that they have less capacity than the surrounding timber members and connections while maintaining effective energy dissipation. Several strategies can be employed to control the shear capacity of the links, including perforated replaceable links [16], low-yield steels [17], built-up sections [6], and cast steel sections [18]. These approaches help reduce the probable capacity of the links, making them more compatible with TS-EBF systems.

2.2 CONNECTIONS OF TS-EBF SYSTEM

Seismic energy in traditional timber structures is dissipated through the yielding of ductile connections [19]. For example, a light wood frame shear wall dissipates energy through the yielding of the nails that attach the sheathing to the timber frame [20]. However, these timber connections are prone to significant strength and stiffness degradation (pinching) during cyclic loading due to joint loosening. In recently developed timber-steel hybrid SFRSs [3–5], ductile elements (e.g., steel BRB and steel links) are systematically included in the system to dissipate energy, whereas other connections are capacity-protected. Connections with high capacity are required to restrict the inelastic deformations to the energy-dissipating members. Many researchers have proposed innovative connections and conducted experiments to validate their capacity. Gilbert et al. [21] developed a high-capacity glue-in-rod connection for high-performance friction-damping devices, BRBs, and

https://doi.org/10.52202/080513-0369

other high-performance braces. Their half-scale laboratory experiments demonstrated that the timber members and connections remained elastic up to a 4.4% equivalent drift. Dong et al. [4] used dowel connections with knife plates and screwed connections with steel side plates to create strong, stiff, and tight moment connections for glulam beam-column joints. The connections had higher strength and stiffness to efficiently engage the BRBs to resist lateral loads. Moerman et al. [5] tested bolted, self-drilling dowels, and screwed connections for coupled CLT shear walls with steel links. A layer of cementitious grout is poured between the steel end plate and the CLT notch surfaces to create a tight connection. Dowel and self-tapping screw connections are recommended for TS-EBFs due to their proven structural performance and wide availabilty. In addition, glued-in rods can be utilized at link-to-beam connections to enhance moment transfer efficiency.

2.3 ELASTIC COMPONENTS OF THE TS-EBF SYSTEM

All TS-EBF components other than the link must remain elastic under earthquake action. These elements are designed for the capacity of the yielded and strain-hardened link, where the yield force of the link is scaled by an overstrength factor that accounts for the probable yield stress exceeding the minimum specified value.

Elastic steel extensions are placed at both ends of the link to prevent direct contact between the plastically deformed steel link and the timber members. These steel beam segments are designed to resist forces corresponding to the probable resistance of the link, whereas the timber beam segments and connections are designed for forces corresponding to the yielding capacity of the elastic steel extensions. This configuration enables the steel extension to act as a secondary failure mechanism, ensuring that any unexpected yielding occurs in the steel extension rather than the timber members, thereby preventing brittle failure. In addition, these steel extensions serve as connection points for beam-brace joints.

Diagonal braces and their connections must be designed to resist axial forces corresponding to the capacity of the elastic steel extensions. The columns of the TS-EBF are designed to withstand both the forces from the elastic steel segment and the gravity loads. Because not all links yield at full capacity simultaneously, column design can use a lower strain-hardening factor than braces and beams, except for the top two storeys [12], where a different factor applies.

3. NUMERICAL MODELLING OF TS-EBFs

Two-dimensional numerical models of the TS-EBF system were developed in *OpenSeesPy* (Figure 1c). The model utilizes a force-based fiber element to simulate the axial and flexural behaviour of the link, combined with the *Steel4* material model in *OpenSeesPy* to capture the shear behaviour. The *Steel4* material incorporates combined kinematic and isotropic hardening and includes an option to account for a non-symmetric force-deformation hysteresis. The material model was calibrated using experimental data from perforated web EBF links tested by Li et al. [16].

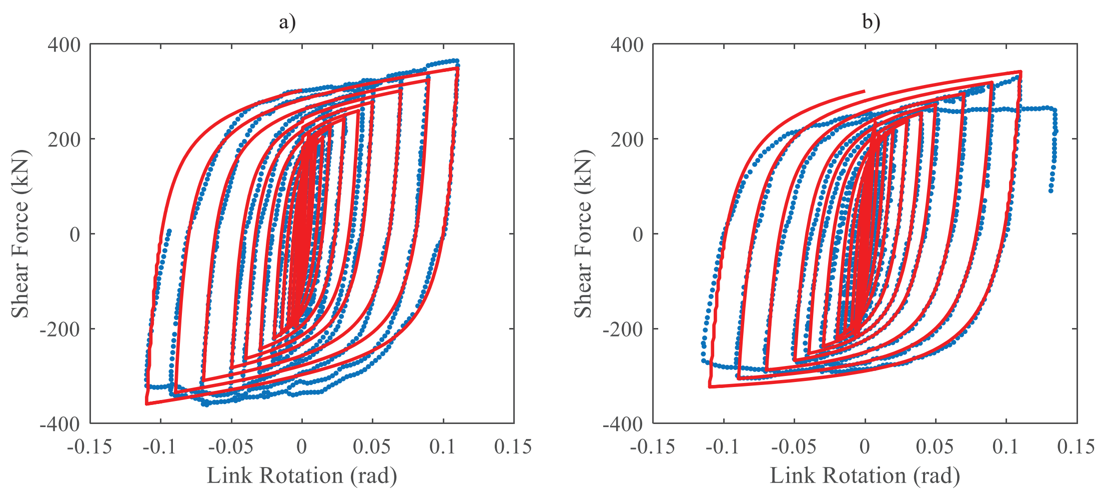

Figure 2. Component level validation: a) link without web perforation; b) link with 50 mm web perforation; test data from Li et al. [29].

The yield force used in the material model corresponds to the link yield force $V_y = 0.55F_yA_v$, with an initial stiffness of GA_v, where F_y and G are the yield stress and shear modulus of steel, respectively, and A_v is the shear area of the link, accounting for area reduction due to web perforations. The post-yield hardening ratio is set to $b_k = 0.004$, with elastic-plastic transition parameters $R_0 = 10$, $r_1 = 0.9$, and $r_2 = 0.15$ applied in both compression and tension zones. The isotropic hardening parameters used are: an initial hardening ratio of $b_i = 0.004$, a saturated hardening ratio of $b_l = 0.0001$, an intersection position control parameter $\rho_i = 1.333$, and an exponential transition parameter $R_i = 0.4$. The ultimate strength limit is set as $F_u = 1.5V_p$,with an exponential transition factor $R_u = 4$ to model the transition from kinematic hardening to a perfectly plastic asymptote.

A comparison between the fiber-based model using these calibrated parameters and the experimental data [16] is shown in Figure 2. The numerical model reasonably captures the experimental behaviour, validating the selected parameters.

The validated fiber-based model of the link was then integrated into a multistorey TS-EBF system. The schematic of the *OpenSeesPy* model is shown in Figure 1c. In the multistorey model, the beam-column joints were considered as pin connections due to the limited moment-resisting capacity of timber connections. The pin connection was simulated using a zero-length spring with minimal rotational stiffness. In contrast, the connections between the link and the link extension, as well as between the link extension and the timber beam, were modeled as continuous beams. As shown in Figure 1c, the brace ends are modeled as pin connections, meaning that the braces carry only axial loads and are represented using truss elements. The elastic steel extensions, beams, and columns were modeled using *elasticBeamColumn* elements, with each element assigned its specific cross-section and material properties. To account for the P-Δ effect, a leaning column was connected to the TS-EBF using a highly rigid bar. This accounts for additional moments induced by axial loads acting on laterally displaced gravity columns.

4 – SEISMIC DESIGN OF TS-EBFs

A brief outline of the seismic design procedure for TS-EBFs is provided herein. The traditional code-based or force-based seismic design (FBSD) method relies on seismic force modification factors (SFMFs) to account for the ductility and overstrength of the system. However, these factors are not readily available for novel systems such as TS-EBFs, making it challenging to apply FBSD directly to innovative building designs. Therefore, in this study, a direct displacement-based design (DDBD) approach is proposed as a more generalized and robust methodology for the seismic design of TS-EBFs. The proposed procedure is adapted from the work of Sullivan [22] and O'Reilly and Sullivan [23] on the DDBD of steel EBFs.

One could argue that the ductility of TS-EBFs comes from the steel link, making the response similar to that of steel EBFs. Therefore, the SFMF for steel EBFs, with a ductility-related (R_d) modification factor of 4.0 and an overstrength-related (R_o) modification factor of 1.5 could be applied. However, this cannot be conclusively determined without a comprehensive study to confirm the response. Significant differences arise in the system due to material variations and connection details, making TS-EBFs fundamentally distinct from traditional steel EBFs.

4.1 DIRECT DISPLACEMENT-BASED SEISMIC DESIGN

The core principle of DDBD is to ensure that a structure meets a predefined performance level under a given seismic demand by directly controlling displacements and deformations [24]. The DDBD procedure relies on a substitute structure concept, where a multi-degree-of-freedom (MDOF) system is represented as an equivalent single-degree-of-freedom (SDOF) system. This equivalent system is characterized by its design displacement, Δ_d , effective mass, M_e , and effective height, H_e, calculated as (1), (2), and (3), respectively. where m_i and Δ_i represents the lumped mass and displacement at the i^{th} floor; h_i is the height of the i^{th} storey from the ground, and n is the total number of storeys:

$$\Delta_d = \frac{\sum_{i=1}^{n} m_i \Delta_i^2}{\sum_{i=1}^{n} m_i \Delta_i} \tag{1}$$

$$M_e = \frac{\sum_{i=1}^{n} m_i \Delta_i}{\Delta_d} \tag{2}$$

$$H_e = \frac{\sum_{i=1}^{n} m_i \Delta_i h_i}{\sum_{i=1}^{n} m_i \Delta_i} \tag{3}$$

The DDBD approach requires the displacement profile and the design displacement at the performance limit state, the estimation of a yield displacement to obtain the displacement ductility, and the relationship between equivalent viscous damping (EVD) and ductility [24]. The total yield drift of the system is estimated as the sum of yield deformations of the TS-EBFs components (4): flexural and shear deformation of the beam including the link ($\theta_{beam,i}$), the axial deformation of braces ($\theta_{br,i}$) and columns ($\theta_{col,i}$) [22].

$$\theta_{y,i} = \theta_{link,i} + \theta_{br,i} + \theta_{col,i} \tag{4}$$

The yield drift of the beam is calculated from the vertical deflection of the beams at the yielding point of the link. Yielding deflection, δ_v, is determined using (5), where EI and GA are flexural and shear rigidity, while subscripts "s" and "t" represent the steel link and timber beam outside the link region.

$$\delta_v = (0.55F_y A_v)e\left(\frac{e(L_b - e)^2}{24L_b E_s I_s} + \frac{e^2(L_b - e)}{24L_b E_t I_t} + \frac{1}{2GA_v}\right) \tag{5}$$

Subsequently, the yield drift components of the beams and link are obtained using (6):

$$\theta_{link,i} = (2\delta_{v,i})/(L_b - e_i) \tag{6}$$

The deflection equation is derived under the assumption that the beam is simply supported between the column and the link center, with a concentrated load applied at the brace-beam connection. The concentrated load is equal to the vertical component of the brace reaction when the link reaches its yield strength. The beam is

https://doi.org/10.52202/080513-0369

continuous, with a timber section from the column to the brace working point and a steel section from the brace working point to the center of the link.

The yield drift components due to brace and column deformations are then computed using Equations (7) and (8), respectively, assuming average strain ratios for the braces (k_{br}) and columns (k_{col}). The average strain ratios are design choices, with an initial value of 0.25 suggested by Sullivan [22] for steel EBFs and 0.4 for the hybrid buckling restraint glulam frame suggested by Dong et al. [25]:

$$\theta_{br,i} = (2k_{br,i}\varepsilon_y)/\sin(2\alpha_i) \quad (7)$$

$$\theta_{cols,i} = \left(2k_{cols,i-1}\varepsilon_y(h_i - h_s)\right)/L_b \quad (8)$$

where ε_y is the yield strain of the element determined by (9), h_i is the height of the storey from the base, h_s is the storey height at level i, and $k_{br,i}$ and $k_{br,i}$ are as given in Equations (10) and (11).

$$\varepsilon_{br} = k_{br}\,\varepsilon_y \quad (9)$$

$$k_{br} = P_{f,br,i}/P_{r,br,i} \quad (10)$$

$$k_{col,i-1} = \textstyle\sum_1^{i-1}\left(P_{(f,col,i)}/P_{r,col,i}\right) \quad (11)$$

These three drift components are summed to obtain the total yield drift, as indicated in (4). The plastic drift capacity of each storey is calculated from the plastic link rotation of 0.08 rad for short links. The total storey drift capacity for structural elements is the sum of the total yield drift and plastic drift, $\theta_{c,str,i} = \theta_{y,i} + \theta_{p,i}$.

The critical storey drift limit (θ_c) is identified by comparing the structural storey drift capacity with the interstorey drift limit for non-structural elements, $\theta_{c,non\,str,i}$ typically 2.5%. Using the critical storey drift limit, which is the minimum of $\theta_{c,str,i}$ or $\theta_{c,nstr,i}$, the displacement profile for the selected performance limit state is obtained through (12):

$$\Delta_i = \begin{cases} \theta_c H_i & \text{for } \theta_c \leq \theta_y \\ \theta_c H_i + (\theta_c - \theta_y) H_i \frac{2H_n - H_i}{2H_n - H_1} & for\ \theta_c > \theta_y \end{cases} \quad (12)$$

where θ_y and θ_c are the minimum yield and capacity drift calculated over the entire height of the structure. Sullivan [22] compared this expression with the displacement profiles from the shaking table results and found better matching than the first mode response. The design displacement profile is then scaled by a factor, ω_θ, in (13) to account for the higher mode effects:

$$\omega_\theta = \begin{cases} 1 \text{ for } n \leq 6 \\ 1.24 - 0.04\,n \text{ for } 6 < n \leq 16 \\ 0.6 \text{ for } n > 16 \end{cases} \quad (13)$$

Ductility demands at each storey are then determined using (14):

$$\mu_i = \theta_i/\theta_{y,i} = (\Delta_i - \Delta_{i-1})/\left(\theta_{y,i}(h_i - h_{i-1})\right) \quad (14)$$

Traditional DDBD uses equivalent viscous damping (EVD) and a damping-dependent displacement scaling factor to estimate structural displacements from the effective period. However, using separate η and EVD expressions introduce sensitivity to the characteristics of the ground motions. Pennucci et al. [26] proposed eliminating the intermediate EVD term by directly relating η to ductility. They found that η calibrated directly from ductility remained relatively unaffected by variations in ground motion characteristics. The displacement reduction factor at each storey, η_i, is calculated using an equation calibrated by O'Reilly and Sullivan [23] for steel EBFs and given in (15).

$$\eta_i = \begin{cases} 1 & \text{for } \mu \leq 1 \\ 2.13\,e^{-1.6\mu_i} + 0.56\,e^{0.01\mu_i} & \text{for } \mu > 1 \end{cases} \quad (15)$$

This equation may be modified in the future to better account for material differences in TS-EBFs. The system displacement reduction factor, η, is calculated from the products of the storey shear proportions and design storey drifts, as indicated in (16).

$$\eta = \frac{\sum_{i=1}^{n} V_i\theta_i\eta_i}{\sum_{i=1}^{n} V_i\theta_i} \quad (16)$$

Because the base shear is not determined yet, a unit base shear is used to establish an equivalent lateral force distribution and the subsequent shear profile.

The design displacement spectrum is scaled by η as in (17), and the effective period is obtained from the scaled spectrum. Next, the substitute structural characteristics, design displacement, effective mass, and effective height are calculated using (1), (2), and (3), respectively.

$$S_{d,in}(T_e) = \eta\,S_d(T) \quad (17)$$

The required effective stiffness, K_e, is estimated from the effective mass and effective period using (18), after which the base shear,V_b, is determined through (19). The P-delta stability coefficient for the system is included in the base shear equation where C is the P-Delta force adjustment factor. If the stability coefficient is less than 0.05, the design base shear does not need amplification to account for P-Delta effects; otherwise, amplification is applied as in (19):

$$K_e = (4\pi^2 M_e)/T_e^2 \quad (18)$$

$$V_b = K_e\Delta_d + C\left(\textstyle\sum_{i=1}^{n} P_i\,\Delta_i\right)/H_e \quad (19)$$

The design base shear is then distributed as a set of equivalent lateral forces, F_i, according to the code (NBCC, 2020 [27]) provided equations. A concentrated load, F_t, equal to $0.07TV_b$ is considered at the top storey to account for the higher mode effect when the fundamental period of the structure exceeds 0.7 s, and the remainder, $V_b - F_t$, is distributed along the height of the building as in (20):

$$F_i = (V_b - F_t)W_i h_i / (\sum_{i=1}^{n} W_i h_i) \qquad (20)$$

The link design shear forces, $V_{link,i}$, are determined from equilibrium using (21), and the link shear resistance at the design drift level, $V_{r,link,i}$, is determined from (22):

$$V_{link,i} = V_i(h_s/L_b) \qquad (21)$$

$$V_{r,link,i} = \begin{cases} (\theta_i/\theta_{y,i})V_{P,link,i} & \text{for } \mu \le 1 \\ \left(1 + 0.25(\gamma_{p,i}/\gamma_p)\right)V_{P,link,i} & \text{for } \mu > 1 \end{cases} \qquad (22)$$

where $V_{P,\mathrm{link,i}}$ is the plastic shear resistance of the link according to the CSA S16-24 [12], $\gamma_{p,u}$ represents the ultimate chord rotation capacity of the link (0.08 rad for short links), and $\gamma_{p,i}$ denotes the expected plastic chord rotation demand at level i, which can be estimated from (22):

$$\gamma_{p,i} = (\theta_i - \theta_{yi})L_b/e_i \qquad (22)$$

The capacity demand ratio of 1.25 is recommended by Sullivan [22] to provide a uniform distribution of strength over the height. Once the links have been designed, the probable capacities of the links are estimated for the design of elastic elements of TS-EBFs. Once the member design has been completed, the actual k_{br} and k_{col} should be checked so that they remain within allowable margins.

4.2 CAPACITY-BASED DESIGN

In TS-EBFs, elements outside the yielding element should sustain the forces, accounting for the probable yield stress exceeding the minimum specified value and the strain hardening. This ensures that the TS-EBF remains elastic, enabling the structure to be reused after an earthquake. The beam segments outside the link, including the connection, must be designed to resist the shear force and bending moments from the strain-hardened link. Similarly, the diagonal braces and their connections must withstand the axial forces resulting from the strain-hardened link plus the reaction from the outside segments of the beam. The columns must be designed to withstand the combined effect of yielding links and gravity loads, but with lower strain-hardening factors than braces and beams, because the cumulative impact of multiple yielding links is generally less than their combined peak forces [6].

5. CASE STUDY BUILDING DESIGN AND SEISMIC PERFORMANCE ASSESSMENT

This section presents a case study building located in a highly seismic region of Canada (Victoria, British Columbia) with a soil classification of type C, designed according to the procedure outlined in Section 4. The seismic performance of the designed building was then assessed using nonlinear static analysis and nonlinear response history analysis. The archetype building is an office building with a typical floor plan and elevations shown in Figure 3. The floor plan consists of three and six regular structural grids measuring 5 m from center to center (Figure 3a). The first storey has a height of 4 m, while each of the upper five storeys has a floor-to-floor height of 3.2 m, resulting in a total building height of 20 m (Figure 3b). The gravity load-resisting system consists of CLT floors and roof, and one-way purlins span between Glulam beams beneath the CLT panels, Glulam beams, and columns.

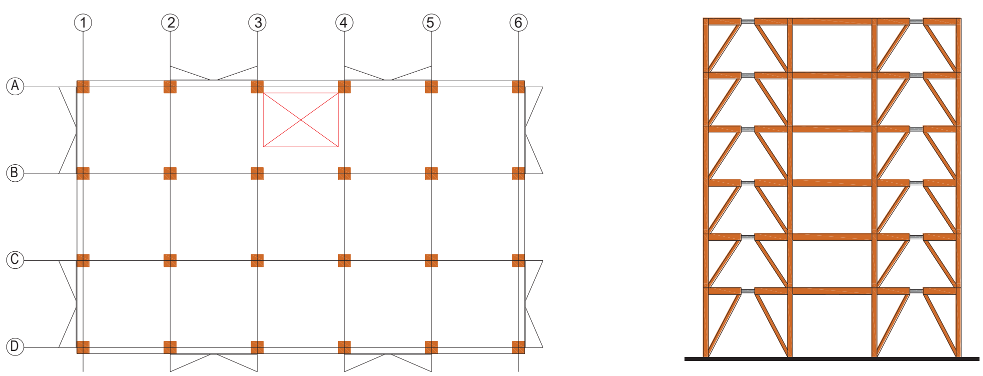

a) b)

Figure 3. Building layout with TS-EBF system: a) floor plan and b) elevation view

https://doi.org/10.52202/080513-0369

5.1 SEISMIC DESIGN OF ARCHETYPE BUILDING

The SFRS of the building consisted of four TS-EBFs in each direction, placed at symmetric locations to minimize torsional effects. The gravity loads and seismic weights were calculated according to the NBCC 2020 [27] guidelines, resulting in a weight of 773 kN at the roof, 1197 kN at the first floor, and 1213 kN at the remaining floors. The DDBD parameters for this building, obtained following the procedure outlined in Section 4, are summarized in Table 1. The controlling storey drift for the displacement profile was 2%, which occurred at the first storey.

Table 1: DDBD design parameters

Design displacement, Δ_d	0.199 m
Effective mass, M_e	154 Ton
Effective height, H_e	13.2 m
System design ductility, μ	2.64
Displacement reduction factor, η	0.719
Effective period, T_e	1.11 s
Design base shear, V_b	995 kN

The seismic base shear obtained from the DDBD (995 kN) was one-quarter of the building's total base shear and was used to design a single TS-EBF. The distribution of this base shear throughout the building height, along with the resulting link demands and corresponding section properties, is summarized in Table 2.

A consistent link length of 950 mm was adopted at all storey levels to improve construction workability and to enhance aesthetics. All link sections were designed to ensure shear-critical behaviour upon yielding. However, the available W-sections, as listed by the Canadian Institute of Steel Construction (CISC), did not provide an optimal design for the elastic members at the upper storeys. To address this, 50 mm perforations were introduced in the webs of the link sections at the top storey to achieve the desired behaviour. Although alternative sections with lower shear capacity were available, they required significantly shorter link lengths to maintain shear-critical behaviour. However, reducing the link length substantially decreased the drift at which the link reaches its ultimate rotation capacity (0.08 rad). This led to a design that was controlled by the local failure of links, which adversely affected overall system performance.

Once the link design was finalized, the timber components of the TS-EBF were designed following CSA O86-24 [19] for the corresponding demands at the ultimate probable resistance of the link section.

Table 2: Archtype building seismic force distribution and TS-EBF design

Level	Storey shear, V_i (kN)	Link shear, $V_{f,link,i}$ (kN)	Link	Link shear resistance, $V_{r,link}$(kN)	$\frac{V_{r,link}}{V_{f,link}}$	Beam	Column	Brace
6	248	159	W250×58	162	1.022	265 × 266	215 × 228	215 × 228
5	461	295	W310×60	335	1.137	315 × 342	215 × 228	265 × 266
4	650	416	W310×60	449	1.080	315 × 380	365 × 342	315 × 342
3	807	516	W310×67	567	1.100	365 × 418	365 × 342	365 × 342
2	924	591	W310×67	624	1.056	365 × 494	365 × 570	365 × 418
1	995	796	W360×91	890	1.119	365 × 608	365 × 570	365 × 532

5.2 NONLINEAR STATIC PUSHOVER ANALYSIS

A nonlinear static pushover analysis (NLSA) was conducted for the archetype building. The structure was pushed in its first eigenmode shape up to 5% roof drift using a displacement-controlled integrator. The roof drift–base shear response, shown in Figure 5a, illustrates the building's global nonlinear behaviour initiating at about 0.55% roof drift and at 1000 kN base shear, which closely aligns with the DDBD design base shear.

5.3 NONLINEAR RESPONSE HISTORY ANALYSIS

Nonlinear response history analysis (NLRHA) was performed to assess the seismic performance of a six-storey TS-EBF SFRS. A selection of ground motion records, representing the complex seismic and tectonic conditions of Victoria, BC, was done, accounting for three primary earthquake sources: shallow crustal, offshore megathrust interface, and deep inslab events. In total, 33 ground motions were chosen, with 11 records from each source type. The crustal and inslab records were obtained from the PEER NGA-West2 database, and the interface earthquake records were sourced from PEER NGA-Sub.

The structure's fundamental period obtained from the dynamic analysis was 0.86 s. The selected ground motions were scaled according to the NBCC-2020 recommendation [27] to match the uniform hazard spectrum (UHS) within the 0.1 s to 5 s period range. Scaling factors of 0.5 to 4 were applied to minimize excessive modifications. As shown in Figure 4, the mean spectrum closely aligns with the UHS across both the fundamental and effective periods of the archetype building.

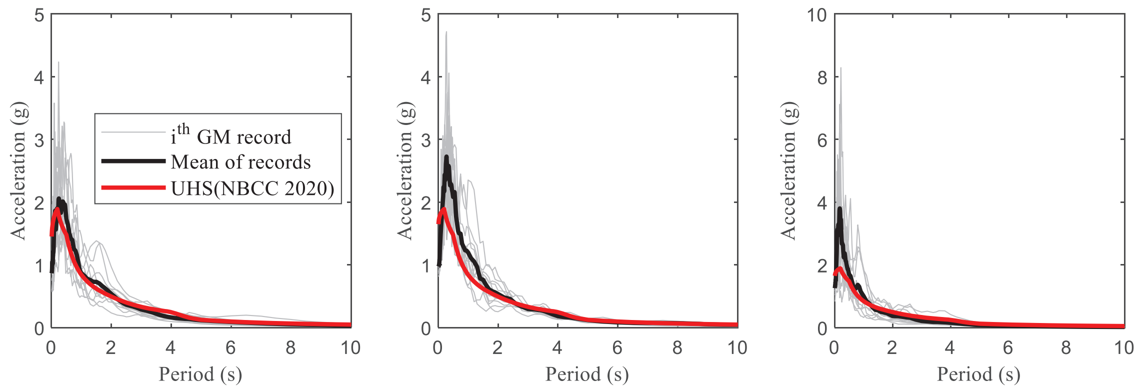

Figure 4. Selected and scaled ground motions; a)Crustal, b) Interface, c) Inslab sources

The NLRHA results, shown in Figures 5b, c and d, indicate that the maximum inter-storey drift ratios (ISDRs) remained below the 2.5% limit specified by the 2020 National Building Code of Canada [27], except for three outliers at the first storey and one at the second storey. The 84th percentile of the NLRHA results closely aligned with the displacement profile obtained from the DDBD approach. This indicates that the proposed design method can effectively achieve the required performance.

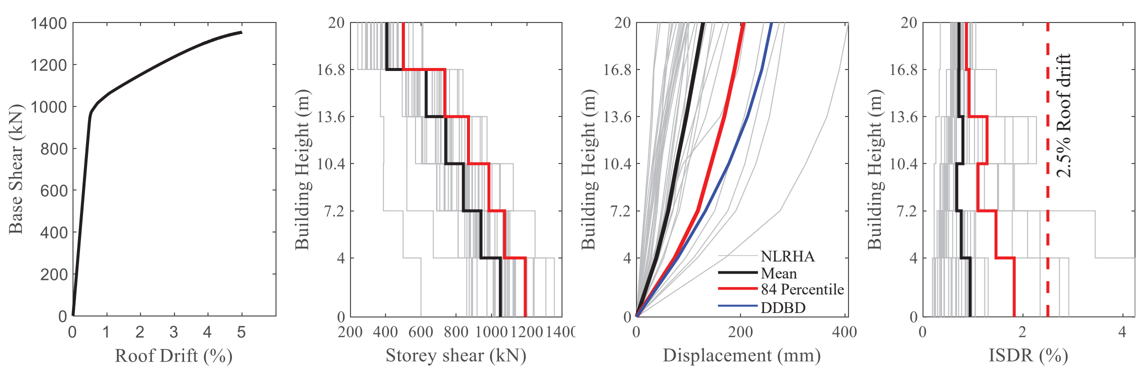

Figure 5. Response of six-storey TS-EBF building; a) NLSA result b) Storey shear response, c) displacement response, d) ISDR procedure

6 – CONCLUSION

The development of a novel hybrid timber-steel eccentrically braced frame (TS-EBF), which combines a ductile steel link with elastic mass timber elements, has been presented in this paper. The first part of the study introduces the system and its characteristics, followed by the development of a procedure specifically tailored for TS-EBFs. To evaluate the seismic response of the system and the effectiveness of this design approach, an archetype building incorporating the TS-EBF as its SFRS was designed and assessed through nonlinear static and response history analyses. The results demonstrated that the DDBD procedure effectively controls building drift within code-prescribed limits while maintaining adequate lateral stiffness. Furthermore, the TS-EBF system successfully dissipates seismic energy through the controlled plastic yielding of shear links, thus enhancing overall seismic performance. Further experimental and numerical studies are required to validate the system's performance, refine the design methodology, and develop comprehensive seismic design guidelines for TS-EBFs.

7 – ACKNOWLEDGMENTS

The authors express their gratitude for the financial support provided by the Ministère des Ressources naturelles et des Forêts (MNRF) Gouvernement du Québec (Government of Quebec). The first author is also supported by a McGill Engineering Doctoral Award (MEDA).

https://doi.org/10.52202/080513-0369

8 – REFERENCES

[1] D. Ugalde, J. L. Almazán, H. Santa Maria, and P. Guindos, "Seismic protection technologies for timber structures: a review," European journal of wood and wood products 77 (2019), pp. 173–194.

[2] S. Tesfamariam and S. F. Stiemer, "Special issue on performance of timber and hybrid structures." American Society of Civil Engineers (2014).

[3] R. Gohlich, J. Erochko, and J. E. Woods, "Experimental testing and numerical modelling of a heavy timber moment-resisting frame with ductile steel links," Earthq Eng Struct Dyn 47.6 (2018), pp. 1460–1477.

[4] W. Dong, M. Li, C.-L. Lee, G. MacRae, and A. Abu, "Experimental testing of full-scale glulam frames with buckling restrained braces," Eng Struct 222 (2020), p. 111081.

[5] B. Moerman, M. Li, A. Palermo, T. Smith, and H. Lim, "Cyclic testing and repair of coupled CLT walls with steel link beams," Journal of Structural Engineering 15030 (2024), p. 4023216.

[6] N. Mansour, "Development of the design of eccentrically braced frames with replaceable shear links." PhD thesis. Ubiversity of Toronto, (2010).

[7] S. K. Azad and C. Topkaya, "A review of research on steel eccentrically braced frames," J Constr Steel Res 128 (2017), pp. 53–73.

[8] C. Clifton, M. Bruneau, G. MacRae, R. Leon, and A. Fussell, "Steel structures damage from the Christchurch earthquake series of 2010 and 2011," Bulletin of the New Zealand Society for Earthquake Engineering 44.4 (2011), pp. 297–318.

[9] Michel Bruneau, Chia-Ming Uang, and Rafael Sabelli, Ductile Design of Steel Structures, 2nd Edition. (2011).

[10] A. Filiatrault, Elements of earthquake engineering and structural dynamics, 3rd ed. Presses inter Polytechnique, (2013).

[11] E. P. Popov, K. Kasai, and M. D. Engelhardt, "Advances in design of eccentrically braced frames," Earthquake Spectra 3.1(1987), pp. 43–55.

[12] Canadian Standard Association, CAN/CSA S16-24, Design of steel structures. (2024).

[13] American Institute of Steel Construction, ANSI/AISC 341-22, Seismic Provisions for Structural Steel Buildings. (2022).

[14] European Committee for Standardization (CEN), "EN 1998-1:2004, Eurocode 8, Design of structures for earthquake resistance, part 1: general rules, seismic actions and rules for buildings," (2004).

[15] T. Okazaki and M. D. Engelhardt, "Cyclic loading behavior of EBF links constructed of ASTM A992 steel" J Constr Steel Res 63.6 (2007), pp. 751–765.

[16] S. Li, Y. Zhang, N. Du, B. Wang, and X. Li, "Seismic cyclic test of perforated replaceable link for eccentrically braced frames" Structures 64 (2024), p. 106643.

[17] P. Dusicka, A. M. Itani, and I. G. Buckle, "Cyclic behavior of shear links of various grades of plate steel" Journal of structural engineering 136. 4 (2010), pp. 370–378.

[18] P. Mortazavi, E. Lee, J. Binder, O.-S. Kwon, and C. Christopoulos, "Large-scale experimental validation of optimized cast steel replaceable modular yielding links for eccentrically braced frames" Journal of Structural Engineering, 149.7 (2023), p. 4023071.

[19]Canadian Standard Association, CAN/CSA O86-24, Engineering design in Wood. (2024).

[20] E. Karacabeyli and C. Lum, Technical guide for the design and construction of tall wood buildings in Canada, 2nd ed. FPInnovations (2022).

[21] C. F. Gilbert and J. Erochko, "Development and testing of hybrid timber-steel braced frames" Eng Struct 198 (2019), p. 109495.

[22] T. J. Sullivan, "Direct displacement-based seismic design of steel eccentrically braced frame structures" Bulletin of Earthquake Engineering 11 (2013), pp. 2197–2231.

[23] G. J. O'Reilly and T. J. Sullivan, "Direct displacement-based seismic design of eccentrically braced steel frames" Journal of Earthquake Engineering 20.2 (2016), pp. 243–278.

[24] M. J. N. Priestley, G. M. Calvi, and M. J. Kowalsky, "Displacement Based Seismic Design of Structures," (2007).

[25] W. Dong, M. Li, T. Sullivan, G. MacRae, C.-L. Lee, and T. Chang, "Direct displacement-based seismic design of glulam frames with buckling restrained braces." Journal of Earthquake Engineering 27.8 (2023), pp. 2166–2197.

[26] D. Pennucci, T. J. Sullivan, and G. M. Calvi, "Displacement reduction factors for the design of medium and long period structures" Journal of Earthquake Engineering 15.S1 (2011), pp. 1–29.

[27] National Research Council of Canada, National building code of Canada (2020).

https://doi.org/10.52202/080513-0369